communications physics

Article

https://doi.org/10.1038/s42005-024-01649-y

Resource theory of imaginarity in distributed scenarios

Kang-Da Wu[1,2], Tulja Varun Kondra[3,4], Carlo Maria Scandolo[5,6] ✉, Swapan Rana[7], Guo-Yong Xiang[1,2,8] ✉, Chuan-Feng Li[1,2,8], Guang-Can Guo[1,2,8] & Alexander Streltsov[3,9] ✉

The resource theory of imaginarity studies the operational value of imaginary parts in quantum states, operations, and measurements. Here we introduce and study the distillation and conversion of imaginarity in distributed scenario. This arises naturally in bipartite systems where both parties work together to generate the maximum possible imaginarity on one of the subsystems. We give exact solutions to this problem for general qubit states and pure states of arbitrary dimension. We present a scenario that demonstrates the operational advantage of imaginarity: the discrimination of quantum channels without the aid of an ancillary system. We then link this scenario to local operations and classical communications(LOCC) discrimination of bipartite states. We experimentally demonstrate the relevant assisted distillation protocol, and show the usefulness of imaginarity in the aforementioned two tasks.

Standard quantum theory describes physical reality with complex states, operators, and Hilbert spaces. However, there have always been lots of questions on the role of complex numbers since the early days of quantum physics[1–15]. Recently, the necessity and usefulness of the imaginary part of quantum mechanics have received significant attention[16–25]. Today, quantum mechanics with imaginary numbers seems to be the most successful theory to describe the microscopic world. These research contributions have shown that complex quantum mechanics is fundamentally different from the corresponding real version in many aspects[2,10,13,15,19,26–31], revealing that the imaginary part is not only necessary for the formulation of quantum theory but also plays an important role in many quantum information tasks[9,11,32].

The development of quantum information science over the last two decades has led to a reassessment of quantum properties, such as entanglement[33,34] and coherence[35,36], as resources, which led to the development of quantitative theories that captured these phenomena in a mathematically rigorous fashion[37,38]. Nevertheless, imaginarity had not been studied in this framework until the last few years[16,18,20,21]. In this setting, imaginarity is regarded as a valuable resource that cannot be generated or increased under a restricted class of operations known as real operations (RO). Quantum states whose density matrices (in a fixed basis) contain imaginary parts are viewed as resource states, and thus cannot be created freely by RO.

In this Letter, we study the resource theory of imaginarity in distributed scenarios. (At least) two parties, Alice (A) and Bob (B) are involved and share a bipartite state ρ^{AB}. In this setting, imaginarity is considered a resource only in Bob's system, while Alice can perform arbitrary quantum operations on her system. The duo is further allowed to communicate classically with one another. Overall, we refer to the allowed set of operations in this protocol as local quantum-real operations and classical communication (LQRCC), borrowing the notion from the theory of entanglement[33] and quantum coherence[35]. This framework leads to a variety of problems, which we address and solve in this Letter. In particular, we consider assisted imaginarity distillation, where Alice assists Bob in extracting local imaginarity. If only one-way classical communication is used, we provide a solution to this problem for arbitrary two-qubit states. We also study assisted state conversion, where the goal is to obtain a specific target state on Bob's side. We solve this problem for any target state if Alice and Bob share a

[1]CAS Key Laboratory of Quantum Information, University of Science and Technology of China, 230026 Hefei, People's Republic of China. [2]CAS Center For Excellence in Quantum Information and Quantum Physics, University of Science and Technology of China, 230026 Hefei, People's Republic of China. [3]Centre for Quantum Optical Technologies, Centre of New Technologies, University of Warsaw, Banacha 2c, 02-097 Warsaw, Poland. [4]Institute for Theoretical Physics III, Heinrich Heine University Düsseldorf, Universitätsstraße 1, D-40225 Düsseldorf, Germany. [5]Department of Mathematics and Statistics, University of Calgary, AB T2N 1N4 Alberta, Canada. [6]Institute for Quantum Science and Technology, University of Calgary, AB T2N 1N4 Alberta, Canada. [7]Physics and Applied Mathematics Unit, Indian Statistical Institute, 203 B T Road, Kolkata 700108, India. [8]Hefei National Laboratory, University of Science and Technology of China, Hefei 230088, People's Republic of China. [9]Institute of Fundamental Technological Research, Polish Academy of Sciences, Pawinskiego 5B, 02-106 Warsaw, Poland. ✉e-mail: carlomaria.scandolo@ucalgary.ca; gyxiang@ustc.edu.cn; a.streltsov@cent.uw.edu.pl

pure state initially. Furthermore, we study the role of imaginarity in ancilla-free channel discrimination, showing two real channels that are perfectly distinguishable in the ancilla-free scenario once we allow imaginarity, but become completely indistinguishable if we have access only to real states and real measurements. Additionally, we prove how this task is related to local operations and classical communications (LOCC) discrimination of quantum states, specifically to the LOCC discrimination of their normalized Choi matrices. Finally, we experimentally implement the above protocols in a quantum photonic setup, performing the proof of principle experiment testing the usefulness of imaginarity in such quantum tasks. Our work opens new avenues towards both theoretical and experimental exploration of imaginarity as a quantum resource.

Results and discussion

Resource theory of imaginarity

The starting point of our work is the resource theory of imaginarity, introduced very recently in refs. 16,18,20. The free states in imaginarity theory are identified as real states, which are real density matrices on a given basis $\{|j\rangle\}$. The set of all real states is denoted by $\mathcal{R}$, which can be described by $\mathcal{R} = \{\rho : \langle j|\rho|k\rangle \in \mathbb{R} \text{ for all } j,k\}$. A quantum operation specified by Kraus operators $\{K_j\}$ satisfying $\sum_j K_j^\dagger K_j = \mathbb{1}$, is considered to be free, i.e., real, if it contains only real elements in the chosen basis: $\langle m|K_j|n\rangle \in \mathbb{R}$ for all j,m,n[16,18]. It is known that the set RO coincides with the set of completely non-imaginarity-creating operations[16]. A quantum operation Λ^S is said to be completely non-imaginarity-creating operation if, for every real state $\rho^{S'S}$ the following holds:

$$\mathbb{I}^{S'} \otimes \Lambda^S[\rho^{S'S}] \in R. \tag{1}$$

Here, $\mathbb{I}^{S'}$ is an identity map acting on the system S' and $\rho^{S'S}$ is a state of the system $S' \otimes S$. Moreover, RO coincides with the set of operations that have a real dilation[16]. A quantum operation Λ^S is said to have a real dilation if there exists a real orthogonal matrix O and a real state $\rho^{S'}$ s.t.

$$\Lambda^S(\cdot) = \mathrm{Tr}_{S'}[O(\cdot \otimes \rho^{S'})O^{\mathrm{T}}]. \tag{2}$$

Here, Λ^S is a quantum operation acting on the system S, O is a real orthogonal matrix acting on the system $S' \otimes S$, $\rho^{S'}$ is a real state acting on the system S' and T denotes the transpose operator.

The golden unit, i.e. the maximally resourceful state, is the same in any Hilbert space, regardless of its dimension. In particular, the maximally imaginary states are the two eigenstates of Pauli matrix σ_y,

$$|\hat{\pm}\rangle = \frac{(|0\rangle \pm i|1\rangle)}{\sqrt{2}}. \tag{3}$$

One maximally imaginary qubit is referred to as an imbit in the following.

Now, we will first present some results concerning imaginarity in a single physical system, completing the study in refs. 18,20. Within the framework of quantum resource distillation[38–41], general quantum states can be used for single-shot or asymptotic distillation of imbits via ROs. In the single-shot regime, the answer was already given in refs. 18,20. In particular, the fidelity of imaginarity F_{I}, which quantifies the maximum achievable fidelity between a state ρ and the imbit

$$F_{\mathrm{I}}(\rho) = \max_{\Lambda} F\left(\Lambda[\rho], |\hat{+}\rangle\langle\hat{+}|\right), \tag{4}$$

was used as the figure of merit for single-shot distillation, where $F(\rho,\sigma) = \left[\mathrm{Tr}\left(\sqrt{\sigma}\rho\sqrt{\sigma}\right)^{\frac{1}{2}}\right]^2$. The exact value of fidelity of imaginarity for general ρ was shown to be equal to

$$F_{\mathrm{I}}(\rho) = \frac{1 + \mathcal{I}_{\mathrm{R}}(\rho)}{2}, \tag{5}$$

where $\mathcal{I}_{\mathrm{R}}(\rho) = \min_\tau\{s \geq 0 : (\rho + s\tau)/(1+s) \in \mathcal{R}\}$ is the robustness of imaginarity[18]. When we consider the asymptotic setting, for large n, the fidelity of imaginarity exponentially converges to 1 (for any non-real states). So, it is necessary for us to consider the behavior of the fidelity of imaginarity as a function of n. In particular, the exponent, for large n, is given by $-\log[\mathrm{Tr}(\rho\rho^{\mathrm{T}})^{\frac{1}{2}}]$. For real states, the fidelity of imaginarity is independent of n and is 1/2[42]. More precisely, we can write the fidelity of imaginarity as $F_{\mathrm{I}}(\rho) = 1/2 + ||\rho - \rho^{\mathrm{T}}||_1/4$[18]. If we have n copies of ρ, we can write

$$F_{\mathrm{I}}(\rho^{\otimes n}) = \frac{1}{2} + \frac{1}{4}\left\|\rho^{\otimes n} - \left(\rho^{\mathrm{T}}\right)^{\otimes n}\right\|_1. \tag{6}$$

If ρ is a pure state, i.e., $\rho = |\psi\rangle\langle\psi|$, then we can calculate the fidelity of imaginarity of multiple copies as

$$F_{\mathrm{I}}\left(|\psi\rangle\langle\psi|^{\otimes n}\right) = \frac{1}{2} + \frac{1}{2}\sqrt{1 - |\langle\psi^*|\psi\rangle|^{2n}}. \tag{7}$$

For general states, to see the behavior of $F_{\mathrm{I}}(\rho^{\otimes n})$ with increasing n, we introduce the quantity $P_n(\rho) = 1 - F_{\mathrm{I}}(\rho^{\otimes n})$ representing the minimal infidelity of imaginarity of $\rho^{\otimes n}$. From ref. 43, it follows that the following limit exists and is equal to the quantum Chernoff divergence, denoted as χ, between ρ and ρ^{T}, i.e.,

$$\lim_{n\to\infty} \frac{-\log P_n(\rho)}{n} = \chi(\rho,\rho^{\mathrm{T}}) = -\log\left\{\min_{0\leq s\leq 1} \mathrm{Tr}\left[\rho^s\left(\rho^{\mathrm{T}}\right)^{1-s}\right]\right\}. \tag{8}$$

One can analytically perform this minimization and show that the minimum value is attained at $s = 1/2$. In order to show this fact, let us assume that the spectral decomposition of ρ is given by $\rho = \sum_j p_j|\psi_j\rangle\langle\psi_j|$, and therefore $\rho^{\mathrm{T}} = \sum_j p_j|\psi_j^*\rangle\langle\psi_j^*|$. The Chernoff divergence is given by $\chi(\rho,\rho^{\mathrm{T}}) = -\log(\min_{0\leq s\leq 1}\sum_{j,k} p_j^s p_k^{1-s}|\langle\psi_j|\psi_k^*\rangle|^2)$. Note that, $|\langle\psi_j|\psi_k^*\rangle| = |\langle\psi_k|\psi_j^*\rangle|$. This implies that $\chi(\rho,\rho^{\mathrm{T}}) = -\log[\min_{0\leq s\leq 1}\sum_{j\leq k}(p_j^s p_k^{1-s} + p_k^s p_j^{1-s})|\langle\psi_j|\psi_k^*\rangle|^2]$. here, $p_j^s p_k^{1-s} + p_k^s p_j^{1-s} \geq 2\sqrt{p_j p_k}$. This lower bound (minimum value) is attained at $s = 1/2$. This proves that

$$\chi(\rho,\rho^{\mathrm{T}}) = -\log\left[\mathrm{Tr}\left(\rho\rho^{\mathrm{T}}\right)^{\frac{1}{2}}\right]. \tag{9}$$

Therefore, from Eq. (8), it follows that asymptotically, the fidelity of imaginarity behaves as

$$F_{\mathrm{I}}(\rho^{\otimes n}) \sim 1 - \exp\left[-n\cdot\chi(\rho,\rho^{\mathrm{T}})\right] = 1 - \left[\mathrm{Tr}\left(\rho\rho^{\mathrm{T}}\right)^{\frac{1}{2}}\right]^n. \tag{10}$$

One of the key motivations for us to study the resource of imaginarity is that we can simulate arbitrary operations or measurements with one imbit at hand, even if all devices allow only real ones in our lab. To see this, let us say we want to implement a quantum operation Λ on ρ with Kraus operators given by $\{K_j\}$, such that $\sum_j K_j^\dagger K_j = P \leq \mathbb{1}$. To implement this, we construct a real quantum operation (Λ_{r}) with Kraus operators given by $\{K_j \otimes |\hat{+}\rangle\langle\hat{+}| + K_j^* \otimes |\hat{-}\rangle\langle\hat{-}|\}$. It is easy to see that

$$\Lambda_{\mathrm{r}}(\rho \otimes |\hat{+}\rangle\langle\hat{+}|) = \Lambda(\rho) \otimes |\hat{+}\rangle\langle\hat{+}| \tag{11}$$

and $\sum_j(K_j^\dagger \otimes |\hat{+}\rangle\langle\hat{+}| + K_j^{\mathrm{T}} \otimes |\hat{-}\rangle\langle\hat{-}|)(K_j \otimes |\hat{+}\rangle\langle\hat{+}| + K_j^* \otimes |\hat{-}\rangle\langle\hat{-}|) = P \otimes |\hat{+}\rangle\langle\hat{+}| + P^{\mathrm{T}} \otimes |\hat{-}\rangle\langle\hat{-}| \leq \mathbb{1} \otimes \mathbb{1}$. The last inequality follows from the fact that, $P \leq \mathbb{1} \iff P^{\mathrm{T}} \leq \mathbb{1}$. This shows that one imbit is sufficient to implement general quantum operations. Now we show that there exists a quantum channel, which necessarily requires one imbit, to implement via real operations. As an example, consider the following map (Λ_+)

given by

$$\Lambda_+(\rho) = |\hat{+}\rangle\langle\hat{+}| \text{ for all } \rho. \tag{12}$$

We now show, by contradiction, that the above quantum map requires one imbit to implement. Let us say there is an implementation (with a real operation Λ'_r) such that

$$\Lambda'_r(\rho \otimes \sigma) = \Lambda_+(\rho) = |\hat{+}\rangle\langle\hat{+}| \tag{13}$$

here, if σ is not an imbit and $\rho = |0\rangle\langle 0|$, its easy to see that the state transformation in Eq. (13) is not possible. This is because $\mathcal{I}_g(|0\rangle\langle 0| \otimes \sigma) = \mathcal{I}_g(\sigma) < \mathcal{I}_g(|\hat{+}\rangle\langle\hat{+}|)$.

In entanglement theory, one maximally entangled qubit state (ebit) has a clear operational meaning: it can be used to teleport the state of an unknown qubit deterministically to a remote lab. In imaginarity theory, if all the devices are restricted to implement ROs, e.g., we have only half-wave plate in an optical setup[18,20], we can still prepare arbitrary states or implement arbitrary measurements if we get one imbit at hand.

Bipartite imaginarity theory

The results studied so far concern imaginarity as a resource in a single physical system. We now extend our considerations to the bipartite setting. As mentioned earlier, the task involves a bipartite state ρ^{AB} shared by Alice and Bob, and the goal is to maximize imaginarity on Bob's side under LQRCC. If both parties are restricted to real operations, the corresponding set is called local real operations and classical communication (LRCC)[44]. It is clear that via LQRCC, it is possible to create only states of the form

$$\rho_{qr} = \sum_j p_j \rho_j^A \otimes \sigma_j^B, \tag{14}$$

where ρ_j^A is an arbitrary state on Alice's side, and σ_j^B is a real state on Bob's side. States of this form will be called quantum-real (QR). In the appendix, we show that the choi matrices corresponding to LQRCC are invariant under partial transpose over Bob (Bob is restricted to real operations). This also holds for more general LQRCC maps, which are trace non-increasing. Using this, we now show that, for arbitrary initial state ρ_{AB} and the target pure state $|\psi_{A'B'}\rangle$, the optimal achievable fidelity for a given probability of success p (given by F_p) can be upperbounded by a semi-definite program (SDP).

Theorem 1. *Achievable fidelity for a given probablity of success* $F_p(\rho_{AB} \longrightarrow^{LQRCC} |\psi_{A'B'}\rangle)$, *of transforming* ρ_{AB} into $|\psi_{A'B'}\rangle$ *via LQRCC operations can upper bounded by the following semidefinite program*:

Maximize:

$$\frac{1}{p}\mathrm{Tr}\left(X_{ABA'B'}\,\rho_{AB}^{T} \otimes |\psi_{A'B'}\rangle\langle\psi_{A'B'}|\right) \tag{15}$$

under the constraints,

$$\begin{gathered} X_{ABA'B'} \geq 0, X_{ABA'B'}^{T_{BB'}} = X_{ABA'B'}, \mathrm{Tr}_{A'B'} X_{ABA'B'} \leq \mathbb{1}_{AB} \text{ and} \\ \mathrm{Tr}\left(X_{ABA'B'}\,\rho_{AB}^{T} \otimes \mathbb{1}_{B'}\right) = p. \end{gathered} \tag{16}$$

In the case of LRCC operations, one has to add an additional constraint given by $X_{ABA'B'}^{T_{AA'}} = X_{ABA'B'}$. For the details about the proof, please refer to the "Methods" section. In the special case, when the target state is a local pure state of Bob $|\psi_{B'}\rangle$, one can replace $|\psi_{A'B'}\rangle$ by $|0\rangle \otimes |\psi_{B'}\rangle$, in the objective function.

Assisted imaginarity distillation

Having extended the theory of imaginarity to multipartite systems, we are now ready to present assisted imaginarity distillation. In this task, Alice and Bob aim to extract imaginarity on Bob's side by applying LQRCC operations, which is in analogy to assisted entanglement distillation[45–47] and assisted distillation of quantum coherence[48]. We assume that Alice and Bob share an arbitrary mixed state ρ^{AB}, and the process is performed on a single copy of the state, and only one-way classical communication from Alice to Bob is used. If Alice performs a general measurement $\{M_j^A\}$ on her side, the probability p_j and the corresponding post-measurement state of Bob ρ_j^B are given, respectively, by $p_j = \mathrm{Tr}[(M_j^A \otimes \mathbb{1}^B)\rho^{AB}], \rho_j^B = 1/p_j \mathrm{Tr}_A[(M_j^A \otimes \mathbb{1}^B)\rho^{AB}]$.

As a figure of merit, we now introduce the assisted fidelity of imaginarity, quantifying the maximal single-shot fidelity between Bob's final state and the maximally imaginary state $|\hat{+}\rangle$:

$$F_a(\rho^{AB}) = \max_{\{M_j^A, \Lambda_j\}} \sum_j p_j F\left(\Lambda_j\left[\rho_j^B\right], |\hat{+}\rangle\langle\hat{+}|\right). \tag{17}$$

The maximum is taken over all positive operator-valued measures (POVM) on Alice's side and all real operations Λ_j on Bob's side. For two-qubit states, we can derive the exact analytic expression. Consider a two-qubit state ρ^{AB}, which can be written as

$$\rho = \frac{1}{4}\left(\mathbb{1} \otimes \mathbb{1} + \sum_k a_k \sigma_k \otimes \mathbb{1} + \sum_l b_l \mathbb{1} \otimes \sigma_l + \sum_{k,l} E_{kl} \sigma_k \otimes \sigma_l\right), \tag{18}$$

where the σ_k's are Pauli matrices, $\boldsymbol{a} = (a_1, a_2, a_3)$ and $\boldsymbol{b} = (b_1, b_2, b_3)$ describe local Bloch vectors of Alice and Bob, respectively, and $E_{kl} = \mathrm{Tr}(\sigma_k \otimes \sigma_l \rho)$. Equipped with these tools, we are now ready to give a closed expression for the assisted fidelity of imaginarity for all two-qubit states.

Theorem 2. *For any two-qubit state* ρ^{AB} *the assisted fidelity of imaginarity is given by*

$$F_a(\rho^{AB}) = \frac{1}{2}\left(1 + \max\{|b_2|, |\boldsymbol{s}|\}\right). \tag{19}$$

where the vector $\boldsymbol{s} = (E_{12}, E_{22}, E_{32})$.

The proof is presented in the Supplementary Note 1. Theorem 2 has a few surprising consequences. If a two-qubit state has the property $|b_2| \geq |\boldsymbol{s}|$, then the assisted fidelity of imaginarity coincides with the fidelity of imaginarity of Bob's local state: $F_a(\rho^{AB}) = (1 + |b_2|)/2$. Thus, in this case Bob will not gain any advantage from assistance, as he can obtain the maximal fidelity by performing a local real operation without any communication. For example, let us consider a quantum state shared by Alice and Bob

$$\rho^{AB} = \frac{p}{2}\mathbb{1}^A \otimes |\hat{+}\rangle\langle\hat{+}| + (1-p)|\phi^+\rangle\langle\phi^+| \tag{20}$$

where we have $b_2 = p$ and $s = (0, p-1, 0)$. Then if $p = 1$, then ρ^{AB} is a product pure state, then no matter what Alice does, Bob can always get the maximal imaginary state $|\hat{+}\rangle$. If $1/2 < p < 1$, the state ρ^{AB} has nonzero entanglement, but we have $|b_2| > |\boldsymbol{s}|$. If Alice chooses a projective measurement along $\boldsymbol{\alpha}$, then Bob will get states with Bloch vector $\boldsymbol{b} \pm \boldsymbol{E}^T \cdot \boldsymbol{\alpha}$ with equal probability. Then, the average fidelity with maximally imaginary state reads $\left(|p + (1-p)\alpha_2| + |p - (1-p)\alpha_2|\right)/2$. As we have $1/2 < p < 1, |(1-p)\alpha_2| < p$, then the average fidelity reads p. For all other two-qubit states Theorem 2 provides an optimal procedure for obtaining maximal fidelity of imaginarity on Bob's side. For this, Alice needs to perform a von Neumann measurement in the basis $\{|\psi_0\rangle, |\psi_1\rangle\}$, where $|\psi_0\rangle$ has the Bloch vector $\boldsymbol{s}/|\boldsymbol{s}|$. The outcome of the measurement is communicated to Bob, who leaves his state untouched if the outcome is 0 and otherwise applies the real unitary $i\sigma_2$.

We will now extend our results to stochastic state transformations, where the goal is to achieve a transformation with the maximum possible probability. To this end, we introduce the geometric measure of imaginarity

and the concurrence of imaginarity, presented in refs. 44,49, respectively, as

$$\mathcal{I}_{\mathrm{g}}(\rho)=\frac{1-\sqrt{F(\rho,\rho^{\mathrm{T}})}}{2}, \tag{21a}$$

$$\mathcal{I}_{\mathrm{c}}(\rho)=\max\left\{0,\lambda_1-\sum_{j>1}\lambda_j\right\}, \tag{21b}$$

where $\{\lambda_1,\lambda_2,\dots\}$ are the eigenvalues (in decreasing order) of $\left(\sqrt{\rho}\rho^{\mathrm{T}}\sqrt{\rho}\right)^{\frac{1}{2}}$. With this in place, we now extend this scenario to the bipartite regime where we will show how Alice can assist Bob (ρ^{B}) to get the target state σ^{B} with optimal probability. Now, we use the following parameterization: $\sin^2\alpha=\left[1-\mathcal{I}_{\mathrm{c}}(\rho^{\mathrm{B}})\right]/2$ and $\sin^2\beta=\mathcal{I}_{\mathrm{g}}(\sigma^{\mathrm{B}})$ with $\alpha,\beta\in(0,\frac{\pi}{2})$.

Lemma 3. *For any bipartite pure state ψ^{AB}, the optimal probability of Bob preparing a local state σ^{B}, getting assistance from Alice, is given by*

$$P(\psi^{\mathrm{AB}}\to\sigma^{\mathrm{B}})=\min\left\{\frac{\sin^2\alpha}{\sin^2\beta},1\right\}. \tag{22}$$

The proof of Lemma 3 is presented in the Supplementary Note 2. In ref. 44, the authors provided tight continuity bounds for the geometric measure. Using these bounds, along with Lemma 3, we can provide an analytical expression for the optimal probability of Bob preparing a local state with an allowed error, with assistance from Alice. Similarly, we can also find a closed expression for the optimal achievable fidelity for a given probability of success. The following theorem collects these results.

Theorem 4. *For any bipartite pure state ψ^{AB}, the optimal probability P_{f} of Bob preparing a local state σ^{B}, with a fidelity f via assistance from Alice, is given by*

$$P_{\mathrm{f}}(\psi^{\mathrm{AB}}\to\sigma^{\mathrm{B}})=\begin{cases}1 & \text{for } \alpha-\beta+\gamma\geq 0\\ \frac{\sin^2\alpha}{\sin^2(\beta-\gamma)} & \text{otherwise}\end{cases} \tag{23}$$

where $\gamma=\cos^{-1}\sqrt{f}$.

The optimal achievable fidelity for a given probability of success, p can be expressed as

$$F_{\mathrm{p}}(\psi^{\mathrm{AB}}\to\sigma^{\mathrm{B}})=\begin{cases}1 & \text{for } p\leq\frac{\sin^2\alpha}{\sin^2\beta}\\ \cos^2\left[\beta-\sin^{-1}\left(\frac{\sin\alpha}{\sqrt{p}}\right)\right] & \text{otherwise.}\end{cases} \tag{24}$$

Details of the proof for the above theorem can be found in Supplementary Note 3.

Imaginarity in channel discrimination

We will now discuss the role of imaginarity in channel discrimination. Specifically, here we focus on the variant of channel discrimination, which we call ancilla-free, in that it does not involve an ancillary system (cf. refs. 50,51). It can be regarded as a game where one has access to a black box with the promise that it implements a quantum channel Λ_j with probability p_j. The goal of the game is to guess Λ_j by choosing optimal initial state ρ and POVM $\{M_j\}$, which is used to distinguish the $\Lambda_j(\rho)$'s. Theoretically, the probability of guessing the channel Λ_j correctly is given as

$$p_{\mathrm{succ}}\left(\rho,\left\{p_j,\Lambda_j\right\},\left\{M_j\right\}\right)=\sum_j p_j\mathrm{Tr}\left[M_j\Lambda_j(\rho)\right]. \tag{25}$$

Recently, it has been shown that any quantum resource has an operational advantage in the channel discrimination task[50,51], namely, a resource state ρ (i.e. a quantum state that is not free) outperforms any free σ in a specific channel discrimination task.

Now, we put the above protocol into imaginarity theory by considering the task of discrimination of real channels. To see an advantage, we need imaginarity both in the probe state and in the measurement since, as we show in the following, this task is equivalent to LOCC discrimination of their corresponding normalized Choi states, in which we need imaginarity in the measurements of both particles. Here we demonstrate a clear link between the task of ancilla-free channel discrimination and the task of LOCC discrimination of bipartite states, the latter studied in refs. 4,18,20. Specifically, we consider the following two scenarios:

1. Let $\mathcal{N}$ and $\mathcal{M}$ be two real channels from A to B, chosen with equal probability $\frac{1}{2}$. If we want to discriminate between them in an ancilla-free scenario better than with a random guess, we must find a real state ρ of A and a real POVM element E of B such that $\mathrm{Tr}\left[E\mathcal{N}(\rho)\right]\neq\mathrm{Tr}\left[E\mathcal{M}(\rho)\right]$. Notice that this protocol does not involve any bipartite input states and bipartite effects.
2. Let $\mathcal{N}$ and $\mathcal{M}$ be two real channels from A to B. This time, we bring in the maximally entangled state $\phi^+=|\phi^+\rangle\langle\phi^+|^{AA'}$, between systems A and A' (A' is a copy of A), where $|\phi^+\rangle=\sum_j|jj\rangle/\sqrt{d_A}$, and d_A is the dimension of A. We apply $\mathcal{N}$ and $\mathcal{M}$ only to the A' part of this maximally entangled state. This results in two bipartite states between systems A and B, N^{AB} and M^{AB}, respectively, which are the normalized Choi states of the two channels $\mathcal{N}$ and $\mathcal{M}$. Now consider the task of discriminating between these two bipartite states of AB using only local real measurements. Again, if we want to discriminate between them better than with a random guess, we must find a real POVM element E of system A and a real POVM element F of system B such that $\mathrm{Tr}\left[(E\otimes F)N^{\mathrm{AB}}\right]\neq\mathrm{Tr}\left[(E\otimes F)M^{\mathrm{AB}}\right]$.

In the following, we show that these two scenarios produce the same probabilites when POVMs are applied to states. Note that we can reconstruct the action of a channel on a state from its normalized Choi state: if $\mathcal{N}$ is a channel from A to B, ρ is a state of A, we have that $\mathcal{N}(\rho)$ can be written in terms of the normalized Choi state N^{AB} as

$$\mathcal{N}(\rho^{\mathrm{A}})=d_A\mathrm{Tr}_A\left\{\left[(\rho^{\mathrm{A}})^{\mathrm{T}}\otimes\mathbb{1}^{\mathrm{B}}\right]N^{\mathrm{AB}}\right\}, \tag{26}$$

where d_A is the dimension of the input system A. Thus, if E is a (real) POVM element on B, omitting system superscripts for simplicity, we have

$$\begin{aligned}\mathrm{Tr}\left[E\mathcal{N}(\rho)\right]&=d_A\mathrm{Tr}\left[(\rho^{\mathrm{T}}\otimes E)N\right]\\&=\mathrm{Tr}\left[\left(\frac{1}{\sqrt{d_A}}\rho^{\mathrm{T}}\otimes\frac{1}{\sqrt{d_A}}E\right)N\right].\end{aligned} \tag{27}$$

Note that $\mathbf{0}\leq\frac{1}{\sqrt{d_A}}\rho^{\mathrm{T}}\leq\mathbb{1}$ and $\mathbf{0}\leq\frac{1}{\sqrt{d_A}}E\leq\mathbb{1}$, then $\frac{1}{\sqrt{d_A}}\rho^{\mathrm{T}}$ and $\frac{1}{\sqrt{d_A}}E$ are both valid (real) POVM elements on A and B, respectively. So now we have a LOCC discrimination scenario on the normalized Choi state N^{AB} that yields exactly the same probability as the original ancilla-free channel discrimination scenario.

Conversely, let us consider the LOCC discrimination scenario of normalized Choi states. Let N^{AB} be the normalized Choi state of a channel $\mathcal{N}$ from A to B. If E and F are POVM elements on A and B, respectively, we want to calculate the probability $\mathrm{Tr}\left[(E\otimes F)N^{\mathrm{AB}}\right]$. Note that, assuming $E\neq\mathbf{0}$, $\rho:=\frac{1}{\mathrm{Tr}E}E$ is a valid quantum state, so $\mathrm{Tr}\left[(E\otimes F)N^{\mathrm{AB}}\right]=\mathrm{Tr}\,E\,\mathrm{Tr}\left[(\rho\otimes F)N^{\mathrm{AB}}\right]$. Then, we have

$$\begin{aligned}\mathrm{Tr}\,E\,\mathrm{Tr}_{AB}\left[(\rho\otimes F)N^{\mathrm{AB}}\right]&=\mathrm{Tr}\,E\,\mathrm{Tr}_B\left\{F\,\mathrm{Tr}_A\left[(\rho\otimes\mathbb{1})N^{\mathrm{AB}}\right]\right\}\\&=\frac{\mathrm{Tr}\,E}{d_A}\mathrm{Tr}_B\left[F\mathcal{N}(\rho^{\mathrm{T}})\right]=\mathrm{Tr}\left[F'\mathcal{N}(\rho^{\mathrm{T}})\right],\end{aligned}$$

where we have used Eq. (26), and we have defined $F' := \frac{\mathrm{Tr}\,E}{d_A} F$. Now, ρ^{T} is still a valid quantum state of A, and F' is still a valid POVM element on B because $\frac{\mathrm{Tr}\,E}{d_A} \leq 1$. So now we have an ancilla-free discrimination scenario on the channels associated with the bipartite normalized state that yields exactly the same probability as the original bipartite LOCC discrimination scenario. In this way, we have proven that all probabilities arising in one of the two scenarios can be completely reproduced by the other scenario, so they are, in some sense, equivalent in terms of the probabilities they can generate.

Having established the relation of channel discrimination and local discrimination of their corresponding Choi states, we can see that the advantage of imaginarity in real channel discrimination shows up when both the initial probe state and measurement contain imaginarity. We accomplish this by mapping the ancilla-free channel discrimination scenario into the LOCC state discrimination scenario, using (normalized) Choi matrices, as discussed above. Let us consider the example of a qubit channel $\mathcal{N}$. Note that its (normalized) Choi state can be written as

$$N^{\mathrm{AB}} = \frac{1}{2}\left(\mathbb{1} + \sum_j a_j \sigma_j^{\mathrm{A}} \otimes \mathbb{1}^{\mathrm{B}} + \mathbb{1}^{\mathrm{A}} \otimes \sum_j b_j \sigma_j^{\mathrm{B}} + \sum_{j,k} E_{jk} \sigma_j^{\mathrm{A}} \otimes \sigma_k^{\mathrm{B}}\right), \tag{28}$$

where $i, j \in \{x, y, z\}$, and the σ_j's are Pauli matrices. If $\mathcal{N}$ is a real operation, then we can conclude that the only term containing σ_y must only be $\sigma_y \otimes \sigma_y$. Recall that $\mathrm{Tr}\left[S\sigma_y\right] = 0$ for any real symmetric 2×2 matrix S (cf. ref. 18). For this reason, any POVM element $M^{\mathrm{AB}} = E^{\mathrm{A}} \otimes F^{\mathrm{B}}$, with real symmetric matrices E or F, cannot be used to detect the presence of the $\sigma_y \otimes \sigma_y$ term in a Choi matrix of a real operation. Consequently, there are some real operations that are perfectly distinguishable, but become indistinguishable using an ancilla-free protocol if we only use real states and measurements. However, if we are still restricted to real probe states and measurements, but we allow an ancilla, then the same real operations become perfectly distinguishable again. To understand why, notice that when we allow an ancilla, we can use the state ϕ^+ as probe state for all real operations, thus producing their normalized Choi states. Then the task becomes distinguishing between their Choi states, but without any LOCC constraints (recall that the LOCC constraint comes from the ancilla-free scenario). Removing the LOCC constraint from the discrimination of the Choi states makes the advantage provided by imaginarity disappear. Consequently, with an ancilla, we can perform as well with just real states and measurements as we do with non-real ones.

To better illustrate this idea, we will provide an example of two real channels that cannot be distinguished in the ancilla-free scenario by using only real states and measurements, but they become instead perfectly distinguishable once we have access to imaginarity for states and measurements. To this end, let us consider two real qubit channels prepared with equal probability:

$$\begin{aligned} \mathcal{N} &: \rho \mapsto \tfrac{1}{2}\left(\rho + \sigma_x \sigma_z \rho \sigma_z \sigma_x\right), \\ \mathcal{M} &: \rho \mapsto \tfrac{1}{2}\left(\sigma_x \rho \sigma_x + \sigma_z \rho \sigma_z\right), \end{aligned} \tag{29}$$

where σ_x and σ_z are Pauli matrices. If we input a real state ρ into either of these two channels, they will produce exactly the same output $\mathbb{1}/2$, thus we cannot distinguish them better than making a random guess, even if we allowed imaginarity in our measurements. On the other hand, if imaginarity is forbidden in measurements, no matter how we choose the probe state (even if it is non-real), we cannot still distinguish them at all because the only way to discriminate between the outputs of the two channels would be to perform a measurement associated with the σ_y Pauli matrix. Indeed, if the probe state has an off-diagonal entry ρ_{01} with non-zero imaginary part, wherever the output of $\mathcal{N}$ has $\mathrm{Im}\,\rho_{01}$, the output of $\mathcal{M}$ will show $-\mathrm{Im}\,\rho_{01}$ in its place. Only if we implement a projective measurement of σ_y can we perfectly distinguish these two channels. Therefore, the only way to achieve a success probability better than random guessing is to introduce imaginarity into both the initial state ρ and the measurement.

It is worth noting that the same two channels $\mathcal{N}$ and $\mathcal{M}$ become perfectly distinguishable even with no imaginarity in the probe state and in the measurement if we remove the requirement of ancilla-free discrimination. If we allow an ancilla R, we need to consider a bipartite input state ρ^{RA} and a bipartite POVM $\{M_1^{RA}, M_2^{RA}\}$, with success probability

$$p_{\mathrm{succ}}\left(\rho, \left\{\frac{1}{2}, \Lambda_j\right\}, \left\{M_j\right\}\right) = \frac{1}{2}\sum_{j=1}^{2} \mathrm{Tr}\left[M_j^{RA}\left(\mathcal{I}^R \otimes \Lambda_j\right)\left(\rho^{RA}\right)\right], \tag{30}$$

where $\Lambda_1 = \mathcal{N}$ and $\Lambda_2 = \mathcal{M}$. Now, let us take $\rho^{RA} = \phi^+ = |\phi^+\rangle\langle\phi^+|$, with $|\phi^+\rangle = \frac{1}{\sqrt{2}}(|00\rangle + |11\rangle)$. If we feed ϕ^+ to both channels, we get

$$\begin{aligned} \mathcal{I} \otimes \mathcal{N}(\phi^+) &= \frac{1}{2}\left(|\phi^+\rangle\langle\phi^+| + |\psi^-\rangle\langle\psi^-|\right), \\ \mathcal{I} \otimes \mathcal{M}(\phi^+) &= \frac{1}{2}\left(|\phi^-\rangle\langle\phi^-| + |\psi^+\rangle\langle\psi^+|\right), \end{aligned} \tag{31}$$

where $|\phi^-\rangle = \frac{1}{\sqrt{2}}(|00\rangle - |11\rangle)$, $|\psi^+\rangle = \frac{1}{\sqrt{2}}(|01\rangle + |10\rangle)$, and $|\psi^-\rangle = \frac{1}{\sqrt{2}}(|01\rangle - |10\rangle)$. As noted in ref. 18, these two output states can be perfectly distinguished by the real POVM $\{M_1, M_2\}$, where

$$\begin{aligned} M_1 &= |\hat{+}\rangle\langle\hat{+}| \otimes |\hat{-}\rangle\langle\hat{-}| + |\hat{-}\rangle\langle\hat{-}| \otimes |\hat{+}\rangle\langle\hat{+}|, \\ M_2 &= |\hat{+}\rangle\langle\hat{+}| \otimes |\hat{+}\rangle\langle\hat{+}| + |\hat{-}\rangle\langle\hat{-}| \otimes |\hat{-}\rangle\langle\hat{-}|. \end{aligned} \tag{32}$$

This shows that the two real channels can be distinguished perfectly with the aid of an ancilla, only using real states and real measurements.

Experiments

We experimentally implement the aforementioned assisted imaginarity distillation and channel discrimination protocols. Here, we would like to briefly mention the reason why imaginarity can be studied in the framework of quantum resource theory. It is noted that complex numbers in describing optics, wave mechanics, and quantum physics are universal, but in most cases, the use of complex numbers is no more than a mathematical trick. In quantum mechanics, however, complex numbers play an indispensable role, and recent works show its necessity and operational meanings both theoretically and experimentally[18,19,22,24,25]. From the above reasoning, it is obvious that in quantum optical settings, imaginarity can be regarded as a precious resource.

Now, we need to justify imaginarity as a resource in certain experimental settings. In majority of physical scenarios, complex phases between different energy states naturally appear during the free evolution, while it is not always the case in several practical settings. In standard linear optics, manipulating complex phase between different optical modes (path or polarization), or implementing complex operations, generally need more optical elements. For example, generating an arbitrary real polarization-encoded state (starting from a free state, i.e., either $|H\rangle$ or $|V\rangle$) requires only half-wave plates. The unitary operation $\cos 2\theta\sigma_x + \sin 2\theta\sigma_z$ can be realized by one half-wave plate with an optical axis set to θ with respect to the horizontal axis. While for pure states with complex-valued amplitudes, we need additional quarter-wave plates to control the exact value of phase[20].

The whole experimental setup is illustrated in Fig. 1, which consists of three modules. In Module **A**, two type-I phase-matched β-barium borate (BBO) crystals, whose optical axes are normal to each other, are pumped by a continuous laser at 404 nm, with a power of 80 mW, for the generation of photon pairs with a central wavelength at $\lambda = 808$ nm via a spontaneous parametric down-conversion process. A half-wave plate (HWP) and a quarter-wave plate (QWP) working at 404 nm set before the lens and BBO crystals are used to control the polarization of the pump laser. Two polarization-entangled photons are generated and then distributed through two single-mode fibers, where one represents Bob and the other Alice. Two interference filters with a 3 nm full width at half maximum (FWHM) are placed to filter out proper transmission peaks. HWPs at both ends of the single-mode fibers are used to control the polarization of both photons.

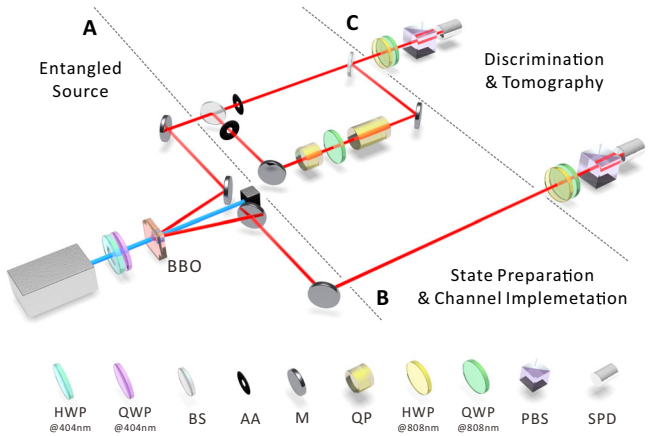

Fig. 1 | Experimental setup. The whole experimental setup is divided into three modules: **A** Entangled source, **B** state preparation & channel implementation, and **C** discrimination & tomography. The optical components include: QP quartz plate, SPD single-photon detectors, BS beamsplitters, AA adjustable aperture, PBS polarizing beamsplitter, QWP quarter-wave plate, HWP half-wave plate, M mirror. @ means working wavelength.

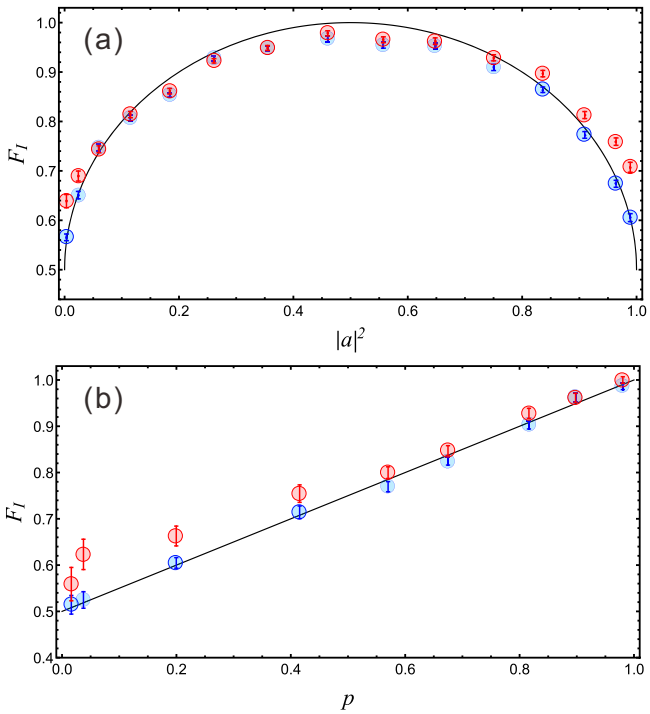

Fig. 2 | Experimental results for assisted imaginarity distillation. a Initial pure states $|\psi\rangle^{AB} = a|00\rangle + b|11\rangle$. **b** Initial Werner states $\rho^{AB} = p|\phi^+\rangle\langle\phi^+| + (1-p)\mathbb{1}/4$. In both experiments, red disks represent the calculated fidelity of imaginarity by assistance using Theorem 2 for experimentally reconstructed two-qubit states, and blue disks represent actual obtained average fidelity of imaginarity in experiments using the optimal measurement on Alice's system. The solid black lines are theoretical predictions for the fidelity of imaginarity by assistance. The error bars are estimated considering the statistical errors due to Poisson distributions of photons.

Overall, module **A** enables us to prepare a two-qubit entangled state via a spontaneous parametric down-conversion (SPDC) process:

$$|\psi\rangle^{AB} = a\,|00\rangle + b\,|11\rangle, \tag{33}$$

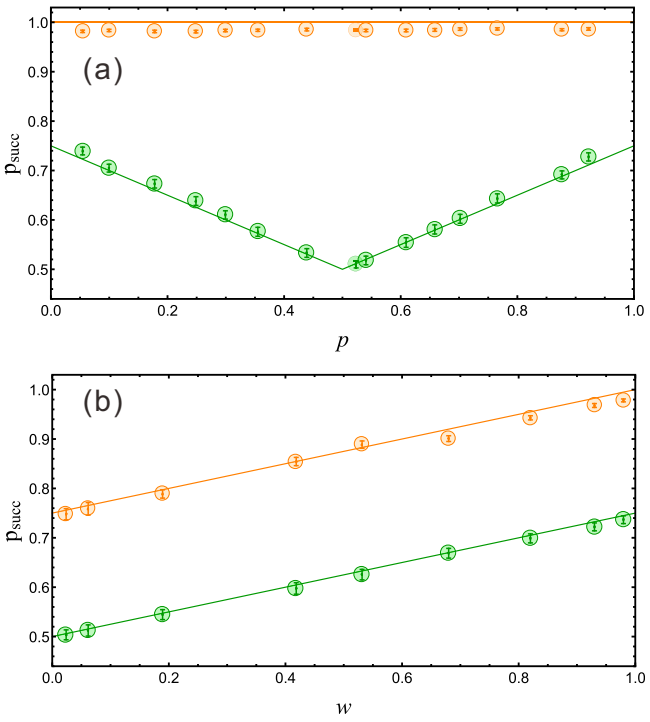

Fig. 3 | Experimental results for discrimination tasks. Two-channel discrimination tasks are tested: **a** $\mathcal{M}_p(\rho) = p\rho + (1-p)\sigma_x\sigma_z\rho\sigma_z\sigma_x, \mathcal{N}(\rho) = (\sigma_x\rho\sigma_x + \sigma_z\rho\sigma_z)/2$. Using imaginarity one can perfectly distinguish the two channels (orange disks). However, if only real operators are allowed, then the optimal guessing probability is $1/2 + |2p-1|/2$ (green disks). **b** $\mathcal{M}_w(\rho) = w\rho + (1-w)\mathbb{1}/2, \mathcal{N}(\rho) = (\sigma_x\rho\sigma_x + \sigma_z\rho\sigma_z)/2$, where optimal distinguishing probabilities are shown with orange and green disks for imaginarity and real case, respectively. The optimal probabilities for successful guessing are $3/4 + w/4$ and $1/4 + w/4$ (see solid orange and green lines) for the case where imaginarity is allowed and where only real states and measurements are allowed, respectively. The error bars are estimated considering the statistical errors due to Poisson distributions of photons.

with arbitrary a and b with $|a|^2 + |b|^2 = 1$ which can be tuned by changing the angles of 404 nm HWP and QWP. Note that we have conventionally set $|0\rangle := |H\rangle$ and $|1\rangle := |V\rangle$. Module **B** utilizes an unbalanced Mach–Zehnder interferometer together with module **A** to prepare a class of Werner states:

$$\rho^{AB} = p\,|\phi^+\rangle\langle\phi^+| + (1-p)\,\frac{\mathbb{1}}{4}, \tag{34}$$

where p denotes the purity of the two-qubit state. Module **B** also allows us to implement single-qubit channels in ancilla-free scenario. For preparing, Werner states, two 50/50 beam splitters (BSs) are inserted into one branch. In the transmission path, the two-photon state is still a Bell state. In the reflected path, three 400λ quartz crystals and a HWP with angles set to 22. 5° are used to dephase the two-photon state into a completely mixed-state $\mathbb{1}^{AB}/4$. The ratio of the two states mixed at the output port of the second BS can be changed by the two adjustable apertures (AA) for the generation of Werner states.

Module **C** allows us to perform quantum-state tomography to identify the final two-qubit polarization-encoded states concerned or perform assisted imaginarity distillation by performing a local measurement on Alice's photons and identifying the exact amount of imaginarity by quantum-state tomography of Bob's state. Moreover, this module allows us

to implement channel discrimination by performing local measurements on the polarization state of a single-photon when the other is used as a trigger.

We then perform proof of principle experiments of the one-shot assisted imaginarity distillation and the ancilla-free channel discrimination tasks. Results are shown in Figs. 2 and 3 respectively.

For assisted imaginarity distillation, we experimentally prepare two classes of two-qubit states. The first class of states as in Eq. (33). Theoretically, the upper bound for single-shot assisted imaginarity distillation can be calculated from Theorem 2 as $F_{\mathrm{I}}(|\psi\rangle^{\mathrm{AB}}) = 2|ab|$. The optimal experimental procedures are as follows: (i) performing a Von Neumann measurement along σ_y on Alice, (ii) Bob's states collapse to $a|0\rangle \pm ib|1\rangle$ corresponding to Alice's measurement outcomes $|\hat{\mp}\rangle$ with an average amount of imaginarity $2|ab|$. From Fig. 2a, we can see that the experimentally obtained average imaginarity after assistance (blue disks) approximately equals to the experimentally obtained upper bound (red disks) within reasonable experimental imperfections. The second class of states is generated as Werner states in Eq. (34). Theoretically, the maximum average fidelity of imaginarity after assistance is calculated as $F_{\mathrm{I}}(\rho^{\mathrm{AB}}) = p$. Experimentally, the optimal amount of imaginarity can be obtained by a similar procedure as done with pure states. Figure 2b details the relevant experimental results. From both results, we see that experimentally obtained average fidelity of imaginarity data and upper bound obtained from two-qubit state tomography agree well with theoretical predictions.

We then show the usefulness of imaginarity in channel discrimination for various discrimination tasks. Figure 3 details these results for two discrimination tasks. The first discrimination task involves two channels given by

$$\begin{aligned}\mathcal{M}(\rho,p) &= p\rho + (1-p)\sigma_x\sigma_z\rho\sigma_z\sigma_x,\\ \mathcal{N}(\rho) &= \frac{1}{2}(\sigma_x\rho\sigma_x + \sigma_z\rho\sigma_z).\end{aligned} \tag{35}$$

Note that the two channels preserve real-density matrices. The experimental results of this discrimination task are shown in Fig. 3a. If we can use imaginarity in measurements and initial states, we can perfectly distinguish the two channels [orange disks in Fig. 3a], agreeing well with theoretical predictions (orange solid lines). In particular, the optimal measurements are performed along $|\hat{\pm}\rangle$ with initial input states $|\hat{+}\rangle$. However, if we allow only real density matrices as initial states or real measurement operators, we get a theoretical optimal guessing probability of $1/2 + |2p-1|/4$ for the ancilla-free channel discrimination. Experimental data are in agreement with the theoretical predictions [see green disks in Fig. 3a and solid lines]. Here we note that the two channels are exactly the same as in Eq. (29) when $p = 1/2$. For the second discrimination task, we consider

$$\begin{aligned}\mathcal{M}(\rho,w) &= w\rho + (1-w)\frac{\mathbb{1}}{2},\\ \mathcal{N}(\rho) &= \frac{1}{2}(\sigma_x\rho\sigma_x + \sigma_z\rho\sigma_z).\end{aligned} \tag{36}$$

The results are shown in Fig. 3b. If non-real states and measurement operators are allowed, then we get a theoretical optimal distinguishing probability as $3/4 + w/4$ (orange solid lines), which is plotted as the upper orange line in Fig. 3b. The relevant experimentally obtained distinguishing probabilities are shown as orange disks. The optimal experimental procedures are similar to the experiments done with states in Eq. (35). If imaginarity is prohibited in this task, then the optimal distinguishing probability reads $1/2 + w/4$, and is plotted as the lower green line (theoretical predictions) together with experimental values represented by green disks. We can draw a similar conclusion to the first discrimination task. In both experiments, the error bars are estimated considering the statistical errors due to Poisson distributions of photons. The possible experimental errors are the uncertainty in the angles of HWPs and QWPs(~0.5°), the noise due to the Poisson distribution of photon numbers, and the phase noise due to mechanical-vibration-induced differences in optical paths.

Conclusion

The results presented above are mainly based on the set of LQRCC operations which was introduced and studied in this article. We considered assisted imaginarity distillation in this setting and completely solved the problem for general two-qubit states. Moreover, we discussed the task of single-shot assisted imaginarity distillation for arbitrary pure states in higher dimensions. The usefulness of imaginarity in channel discrimination is both theoretically and experimentally shown for a class of real channels.

There are, in fact, many scenarios of practical relevance where the task of assisted imaginarity distillation can play a central role. For instance, think of a remote or unaccessible system on which imaginarity is needed as a resource (e.g., in the task of local discrimination of quantum states): our results give optimal prescriptions to inject such imaginarity on the remote target by acting on an ancilla. The results provide insight into both the operational characterization as well as the mathematical formalism of the resource theory of imaginarity, contributing to a better understanding of this fundamental resource.

Methods

Properties of LRCC operations

For any real completely positive (CP) map $\Lambda : R \to R'$, $\Gamma^{\Lambda}_{RR'}$ is the corresponding Choi matrix of $\Gamma^{\Lambda}_{RR'}$, given by

$$\Gamma^{\Lambda}_{RR'} = \mathbb{1}\otimes\Lambda\left(\sum_{j,k}|j\rangle\langle k|\otimes|j\rangle\langle k|\right). \tag{37}$$

Any LQRCC map (Λ) can be represented in the following way:

$$\Lambda = \sum_i \Lambda_i \otimes \Lambda_i^{\mathrm{r}}. \tag{38}$$

Here, λ_i is a CP and trace non-increasing map acting locally on Alice's Hilbert spapce and Λ_i^{r} is a local real CP map on Bob's Hilbert space. The Choi matrix of $\Lambda_i \otimes \Lambda_i^{\mathrm{r}}$ is given by

$$\begin{aligned}\Gamma^{\Lambda_i\otimes\Lambda_i^{\mathrm{r}}}_{AB\to A'B'} &= \mathbb{1}_{AB}\otimes\Lambda_i\otimes\Lambda_i^{\mathrm{r}}\left(\sum_{j,j',k,k'}|jk\rangle\langle j'k'|\otimes|jk\rangle\langle j'k'|\right)\\ &= \sum_{j,j',k,k'}|j\rangle\langle j'|\otimes|k\rangle\langle k'|\otimes\Lambda_i(|j\rangle\langle j'|)\otimes\Lambda_i^{\mathrm{r}}(|k\rangle\langle k'|)\end{aligned}$$

Let's now take the transpose of this choi matrix over BB'

$$\begin{aligned}\left(\Gamma^{\Lambda_i\otimes\Lambda_i^{\mathrm{r}}}_{AB\to A'B'}\right)^{T_{BB'}} &= \sum_{j,j',k,k'}|jk'\rangle\langle j'k|\otimes\Lambda_i(|j\rangle\langle j'|)\otimes\left(\Lambda_i^{\mathrm{r}}(|k\rangle\langle k'|)\right)^T\\ &= \sum_{j,j',k,k'}|jk'\rangle\langle j'k|\otimes\Lambda_i(|j\rangle\langle j'|)\otimes\Lambda_i^{\mathrm{r}}(|k'\rangle\langle k|)\\ &= \Gamma^{\Lambda_i\otimes\Lambda_i^{\mathrm{r}}}_{AB\to A'B'}\end{aligned} \tag{39}$$

In the second line, we used the fact that real operations commute with transpose. Since any LQRCC operation can be represented as Eq. (38), the Choi matrix of any LQRCC operation is invariant under partial transpose over Bob's systems. For LRCC operations, additionally, the Choi matrix is always real.

Semi-definite program upperbounds for state transformations

As we already mentioned, for any real CP map $\Lambda : R \to R'$, $\Gamma^{\Lambda}_{RR'}$ is the corresponding Choi matrix of $\Gamma^{\Lambda}_{RR'}$, given by

$$\Gamma^{\Lambda}_{RR'} = \mathbb{1}\otimes\Lambda\left(\sum_{j,k}|j\rangle\langle k|\otimes|j\rangle\langle k|\right). \tag{40}$$

It follows that (see Eq. (4.2.12) of ref. 52),

$$\Lambda(\rho_R) = \mathrm{Tr}_R(\Gamma^{\Lambda}_{RR'}(\rho_R^{\mathrm{T}} \otimes \mathbb{1}_{R'})). \tag{41}$$

For any pure state $|\psi_{R'}\rangle$

$$\langle\psi_{R'}|\Lambda(\rho_R)|\psi_{R'}\rangle = \mathrm{Tr}(\Gamma^{\Lambda}_{RR'}(\rho_R^{\mathrm{T}} \otimes |\psi_{R'}\rangle\langle\psi_{R'}|)). \tag{42}$$

Using the fact that Choi matrices of LQRCC operations are invariant under partial transpose, one can give a semi-definite program (SDP) computable upperbound for the optimal achievable fidelity for a given probability $F_p(\rho_{AB} \to |\psi_{AB}\rangle)$: Maximize:

$$\frac{1}{p}\mathrm{Tr}(X_{ABA'B'}\rho_{AB}^{\mathrm{T}} \otimes |\psi_{A'B'}\rangle\langle\psi_{A'B'}|) \tag{43}$$

under the constraints

$$\begin{gathered} X_{ABA'B'} \geq 0, X^{\mathrm{T}_{BB'}}_{ABA'B'} = X_{ABA'B'}, \mathrm{Tr}_{A'B'}X_{ABA'B'} \leq \mathbb{1}_{AB} \text{ and} \\ \mathrm{Tr}(X_{ABA'B'}\rho_{AB}^{\mathrm{T}} \otimes \mathbb{1}_{B'}) = p. \end{gathered} \tag{44}$$

Data availability

Raw data are available from the authors upon reasonable request.

Received: 21 April 2023; Accepted: 30 April 2024;
Published online: 31 May 2024

References

1. Jordan, P., von Neumann, J., & Wigner, E. P. On an algebraic generalization of the quantum mechanical formalism. In *The Collected Works of Eugene Paul Wigner: Part A: The Scientific Papers* (ed. Wightman, A. S.) 298–333 (Springer, Berlin, Heidelberg, 1993).
2. Stückelberg, E. C. Quantum theory in real Hilbert space. *Helv. Phys. Acta* **33**, 727 (1960).
3. Araki, H. On a characterization of the state space of quantum mechanics. *Commun. Math. Phys.* **75**, 1 (1980).
4. Wootters, W. K. Local accessibility of quantum states. In *Complexity, Entropy and the Physics of Information* (ed. Zurek, W. H.) 39–46 (Addison-Wesley, 1990).
5. Caves, C. M., Fuchs, C. A. & Rungta, P. Entanglement of formation of an arbitrary state of two rebits. *Found. Phys. Lett.* **14**, 199 (2001).
6. Wootters, W. K. Parallel transport in an entangled ring. *J. Math. Phys.* **43**, 4307 (2002).
7. Batle, J., Plastino, A. R., Casas, M. & Plastino, A. On the entanglement properties of two-rebits systems. *Phys. Lett. A* **298**, 301 (2002).
8. Batle, J., Plastino, A. R., Casas, M. & Plastino, A. Understanding quantum entanglement: qubits, rebits and the quaternionic approach. *Opt. Spectrosc.* **94**, 700 (2003).
9. McKague, M., Mosca, M. & Gisin, N. Simulating quantum systems using real Hilbert spaces. *Phys. Rev. Lett.* **102**, 020505 (2009).
10. Hardy, L. & Wootters, W. K. Limited holism and real-vector-space quantum theory. *Found. Phys.* **42**, 454 (2012).
11. Wootters, W. K. Entanglement sharing in real-vector-space quantum theory. *Found. Phys.* **42**, 19 (2012).
12. Baez, J. C. Division algebras and quantum theory. *Found. Phys.* **42**, 819 (2012).
13. Aleksandrova, A., Borish, V. & Wootters, W. K. Real-vector-space quantum theory with a universal quantum bit. *Phys. Rev. A* **87**, 052106 (2013).
14. Wootters, W. K. The rebit three-tangle and its relation to two-qubit entanglement. *J. Phys. A* **47**, 424037 (2014).
15. Wootters, W. K. Optimal information transfer and real-vector-space quantum theory. In *Quantum Theory: Informational Foundations and Foils* (eds Chiribella, G. & Spekkens, R. W.) 21–43 (Springer, Netherlands, Dordrecht, 2016).
16. Hickey, A. & Gour, G. Quantifying the imaginarity of quantum mechanics. *J. Phys. A* **51**, 414009 (2018).
17. Barnum, H., Graydon, M. A. & Wilce, A. Composites and categories of Euclidean Jordan algebras. *Quantum* **4**, 359 (2020).
18. Wu, K.-D. et al. Operational resource theory of imaginarity. *Phys. Rev. Lett.* **126**, 090401 (2021).
19. Renou, M.-O. et al. Quantum theory based on real numbers can be experimentally falsified. *Nature* **600**, 625 (2021).
20. Wu, K.-D. et al. Resource theory of imaginarity: quantification and state conversion. *Phys. Rev. A* **103**, 032401 (2021).
21. Xue, S., Guo, J., Li, P., Ye, M. & Li, Y. Quantification of resource theory of imaginarity. *Quantum Inf. Process.* **20**, 383 (2021).
22. Chen, M.-C. et al. Ruling out real-valued standard formalism of quantum theory. *Phys. Rev. Lett.* **128**, 040403 (2022).
23. Aberg, J. Quantifying superposition. arXiv:quant-ph/0612146 (2006).
24. Li, Z.-D. et al. Testing real quantum theory in an optical quantum network. *Phys. Rev. Lett.* **128**, 040402 (2022).
25. Wu, D. et al. Experimental refutation of real-valued quantum mechanics under strict locality conditions. *Phys. Rev. Lett.* **129**, 140401 (2022).
26. Sperling, J. et al. Two-rebit entanglement: Theory and experiment. in *Quantum Information and Measurement* (Optica Publishing Group, 2021).
27. Barzi, F. On complex numbers in quantum mechanics. arXiv e-prints, arXiv:2108.05715 (2021), arXiv:2108.05715 [physics.gen-ph].
28. Bednorz, A. & Batle, J. Optimal discrimination between real and complex quantum theories. *Phys. Rev. A* **106**, 042207 (2022).
29. Chen, Q., Gao, T. & Yan, F. Measures of imaginarity and quantum state order. *Sci. China-Phys. Mech. Astron.* **66**, 280312 (2023).
30. Prasannan, N. et al. Experimental entanglement characterization of two-rebit states. *Phys. Rev. A* **103**, L040402 (2021).
31. Roa, L., Muñoz, A., Muñoz, C. & Klimov, A. B. Deterministic entanglement extraction. *Phys. Rev. A* **99**, 052344 (2019).
32. Zhu, H. Hiding and masking quantum information in complex and real quantum mechanics. *Phys. Rev. Research* **3**, 033176 (2021).
33. Horodecki, R., Horodecki, P., Horodecki, M. & Horodecki, K. Quantum entanglement. *Rev. Mod. Phys.* **81**, 865 (2009).
34. Vedral, V., Plenio, M. B., Rippin, M. A. & Knight, P. L. Quantifying entanglement. *Phys. Rev. Lett.* **78**, 2275 (1997).
35. Streltsov, A., Adesso, G. & Plenio, M. B. Colloquium: quantum coherence as a resource. *Rev. Mod. Phys.* **89**, 041003 (2017).
36. Baumgratz, T., Cramer, M. & Plenio, M. B. Quantifying coherence. *Phys. Rev. Lett.* **113**, 140401 (2014).
37. Coecke, B., Fritz, T. & Spekkens, R. W. A mathematical theory of resources. *Inform. Comput.* **250**, 59 (2016).
38. Chitambar, E. & Gour, G. Quantum resource theories. *Rev. Mod. Phys.* **91**, 025001 (2019).
39. Bennett, C. H. et al. Purification of noisy entanglement and faithful teleportation via noisy channels. *Phys. Rev. Lett.* **76**, 722 (1996).
40. Regula, B., Bu, K., Takagi, R. & Liu, Z.-W. Benchmarking one-shot distillation in general quantum resource theories. *Phys. Rev. A* **101**, 062315 (2020).
41. Regula, B., Fang, K., Wang, X. & Adesso, G. One-shot coherence distillation. *Phys. Rev. Lett.* **121**, 010401 (2018).
42. Wu, K.-D. et al. Experimental cyclic interconversion between coherence and quantum correlations. *Phys. Rev. Lett.* **121**, 050401 (2018).
43. Audenaert, K. M. R. et al. Discriminating states: the quantum chernoff bound. *Phys. Rev. Lett.* **98**, 160501 (2007).
44. Kondra, T. V., Datta, C. & Streltsov, A. Real quantum operations and state transformations. *New J. Phys.* **25**, 093043 (2023).

45. DiVincenzo, D. P. et al. Entanglement of assistance. In *Quantum Computing and Quantum Communications*: First NASA International Conference, QCQC'98 Palm Springs, California, USA. 247–257 (Springer Berlin Heidelberg, 1998).
46. Smolin, J. A., Verstraete, F. & Winter, A. Entanglement of assistance and multipartite state distillation. *Phys. Rev. A* **72**, 052317 (2005).
47. Gour, G. & Spekkens, R. W. Entanglement of assistance is not a bipartite measure nor a tripartite monotone. *Phys. Rev. A* **73**, 062331 (2006).
48. Chitambar, E. et al. Assisted distillation of quantum coherence. *Phys. Rev. Lett.* **116**, 070402 (2016).
49. Uhlmann, A. Fidelity and concurrence of conjugated states. *Phys. Rev. A* **62**, 032307 (2000).
50. Takagi, R., Regula, B., Bu, K., Liu, Z.-W. & Adesso, G. Operational advantage of quantum resources in subchannel discrimination. *Phys. Rev. Lett.* **122**, 140402 (2019).
51. Takagi, R. & Regula, B. General resource theories in quantum mechanics and beyond: operational characterization via discrimination tasks. *Phys. Rev. X* **9**, 031053 (2019).
52. Khatri, S. & Wilde, M. M. Principles of quantum communication theory: a modern approach, arXiv:2011.04672 [quant-ph].

Acknowledgements

The work at the University of Science and Technology of China is supported by the National Natural Science Foundation of China (Grants Nos. 12134014, 12104439, 61905234, the Key Research Program of Frontier Sciences, CAS (Grant No. QYZDYSSW-SLH003), USTC Research Funds of the Double First-Class Initiative (Grant No. YD2030002007) and the Fundamental Research Funds for the Central Universities. The work in Poland was supported by the National Science Centre Poland (Grant No. 2022/46/E/ST2/00115) and the "Quantum Optical Technologies" project, carried out within the International Research Agendas program of the Foundation for Polish Science co-financed by the European Union under the European Regional Development Fund. C.M.S. acknowledges the support of the Natural Sciences and Engineering Research Council of Canada (NSERC) through the Discovery Grant "The power of quantum resources" RGPIN-2022-03025 and the Discovery Launch Supplement DGECR-2022-00119. The work of Tulja Varun Kondra is supported by the German Federal Ministry of Education and Research (BMBF) within the funding program "quantum technologies – from basic research to market" in the joint project QSolid (grant number 13N16163).

Author contributions

G.-Y.X. and A.S. conceived the project. K.-D.W. performed the experimental work under the guidance of G.-Y.X., C.-F.L., and G.-C.G. K.-D.W., T.V.K., and S.R. performed the theoretical work under the guidance of C.M.S. and A.S. K.-D.W., T.V.K., C.M.S., and S.R. drafted the manuscript, with revisions from G.-Y.X. and A.S. All authors approved the final version of the manuscript.

Competing interests

The authors declare no competing interests.

Additional information

Supplementary information The online version contains supplementary material available at https://doi.org/10.1038/s42005-024-01649-y.

Correspondence and requests for materials should be addressed to Carlo Maria Scandolo, Guo-Yong Xiang or Alexander Streltsov.

Peer review information *Communications Physics* thanks Alexander Hickey and the other, anonymous, reviewer(s) for their contribution to the peer review of this work. A peer review file is available.